Computational Simulations of Thrombolysis in Acute Stroke: Effect of Clot Size and Location on Recanalisation

Boram Gu[1], Andris Piebalgs[1], Yu Huang[1], Dylan Roi[2], Kyriakos Lobotesis[2], Colin Longstaff[3], Alun D. Hughes[4,5], Rongjun Chen[1], Simon A. Thom[6], Xiao Yun Xu[1,*]

[1]Department of Chemical Engineering, Imperial College London, South Kensington Campus, London, United Kingdom

[2]Imaging Department, Charing Cross Hospital, Imperial College Healthcare NHS Trust, London W6 8RF, United Kingdom

[3]Biotherapeutics Section, National Institute for Biological Standards and Control, South Mimms, Herts, United Kingdom

[4]Institute of Cardiovascular Science, University College London, London, United Kingdom

[5]MRC Unit for Lifelong Health and Ageing at University College London, London, United Kingdom

[6]National Heart & Lung Institute, Imperial College London, Hammersmith Campus, London, United Kingdom

*Corresponding author. Email address: yun.xu@imperial.ac.uk (X.Y. Xu)

Abstract

Acute ischaemic stroke can be treated by intravenous thrombolysis whereby tissue plasminogen activator (tPA) is infused to dissolve clots that block blood supply to the brain. In this study, we aim to examine the influence of clot location and size on lysis pattern and recanalisation by using a recently developed computational modelling framework for thrombolysis under physiological flow conditions. An image-based patient-specific model is reconstructed which consists of the internal carotid bifurcation with the A1 segment of anterior cerebral arteries and M1 segment of middle cerebral arteries, and the M1

bifurcation containing the M2 segments. By varying the clot size and location, 7 scenarios are simulated mimicking thrombolysis of M1 and M2 occlusions. Our results show that initial breakthrough always occurs along the inner curvature of the occluded cerebral artery, due to prolonged tPA residence time in the recirculation zone. For a given occlusion site, lysis completion time appears to increase almost quadratically with the initial clot volume; whereas for a given clot volume, the simulated M2 occlusions take up to 30% longer for complete lysis compared to the corresponding M1 occlusions.

Keywords: Ischaemic stroke; Thrombolytic therapy; Blood clot; Tissue plasminogen activator (tPA); Computational model; Drug transport

1. Introduction

Ischaemic stroke is one of the leading causes of global death and the most common type of stroke [1,2]. It occurs when a cerebral artery is occluded by a blood clot, impairing blood supply to the brain. The blood clot can be removed by different medical procedures, one of which is thrombolytic therapy whereby a fibrinolytic agent, such as recombinant tissue-type plasminogen activator (tPA), is administered to patients to dissolve the clots in their cerebral arteries. However, the use of tPA is limited by bleeding complications due to the fibrin specificity of tPA [2–4]. Furthermore, the effectiveness of thrombolytic treatment is determined by many factors, such as patients' cerebral vasculature (e.g. collateralisation determined by the architecture of the Circle of Willis) [5,6], the location, size and composition of clot and drug dosing regimens. Mechanical thrombectomy is an alternative method which aims to retrieve blood clots and is increasingly adopted following successful clinical trials [7–9]. Despite its benefits and positive outcomes, it has only been applied to patients with large vessel occlusions [10] and its safety and efficacy for small vessel occlusions remain to be answered [11–13]. It has also been reported that thrombectomy performed in combination with thrombolytic therapy may achieve enhanced treatment outcome [14–17]. Therefore, it is necessary to understand how clots would be dissolved upon tPA infusion in different clinical settings.

To do so, we investigate the effects of various factors on the outcome of thrombolysis via computational simulations using a recently developed mathematical modelling platform [18,19] Our multi-level model includes pharmacokinetics and pharmacodynamics (PKPD) for the systemic levels of tPA and fibrinolytic proteins in the plasma, blood flow and drug transport in patient-specific arterial geometry and fibrinolytic reactions within a fibrin clot [19]. The model was used to study the effects of different drug doses and clot density on the level of fibrinolytic proteins and lysis completion time, indicative of the risk of bleeding and treatment efficacy, respectively.

In addition to drug dosage and clot properties, the size and location of clot have been reported to be associated with the likelihood of successful recanalisation and favourable clinical outcomes [20–26]. A number of clinical studies reported that clot lengths in patients with occlusions in their middle cerebral arteries (MCA) were correlated with the success of recanalisation after thrombolytic therapy [20,24,25]. It was observed in almost all studies that very long clots resulted in low recanalisation rates, although a clear cut-off was not identified. A more recent study by Yoo et al. correlated non-recanalisation after intravenous thrombolysis with the volume of clot, instead of its length [26]. They found that the average clot volume in patients with non-recanalisation was significantly larger than that in patients with successful recanalisation, and clot volume $\geq$200 mm^3 was predictive of non-recanalisation.

Attempts were also made to associate the location of occlusion with recanalisation rates and clinical outcomes [21–23,27]. Saqqur et al. (2007) examined stroke patients with various cerebral occlusions, ranging from internal carotid to distal MCA occlusions [23]. Distal MCA occlusions were reported to achieve high recanalisation rates, whereas terminal ICA occlusions resulted in poor recanalisation and clinical outcome possibly due to larger thrombus burden and poor collaterals. Friedrich et al. (2015) analysed over 130 patients with acute MCA occlusions to identify the relation between the distance from the internal carotid bifurcation to the clot front and clinical outcome based on the degree of impairment

and neurological disability caused by stroke [22]. They found that patients with distal occlusions tend to have a more favourable clinical outcome than those with proximal occlusions, and that distal clots are usually shorter than proximal clots.

Due to the combined effects of the size and location of clot in the above mentioned clinical studies, it is not possible to explain the role of each individual factor when acting alone. To this end, we have performed computational simulations using a recently developed multi-level model for thrombolytic treatment in ischaemic stroke by varying the clot size and location, one parameter at a time, while keeping the dosage regimen and initial clot resistance constant. A three-dimensional (3D) patient-specific model is reconstructed from 3D rotational angiography images, which includes the internal carotid bifurcation into the A1 segment of anterior cerebral arteries (ACA) and the M1 segment of middle cerebral arteries (M1), as well as the M1 bifurcation into the M2 segments. Simulated scenarios are divided into two groups: M1 occlusion and M2 occlusion. For each occlusion site, the volume of clot is varied. Lysis completion times for the simulated scenarios are compared, along with haemodynamics variables, the extent of lysis, clot resistance and tPA concentration inside the clot.

2. Methods

2.1 Overview of the computational model

Figure 1 presents an overview of our recently developed computational model [1], which incorporates multi-level physical and biochemical phenomena present in thrombolysis, from macroscopic blood flow and species transport to reactions of clot lysis within a clot, coupled with interactions between the macroscopic transport phenomena and the progression of clot dissolution. Blood flow and mass transport of free phase species are described by the modified Navier-Stokes equations and the convection-diffusion-reactions equations, respectively (Figure 1 (a)). Fibrinolytic reactions kinetics, illustrated in Figure 1 (b) and (c), are coupled with the macroscopic blood flow and species transport models to update the Darcian momentum and reactions source terms as clot lysis takes place. Full details of the

mathematical models of blood flow, species transport and fibrinolytic reaction kinetics can be found in our previous work [19].

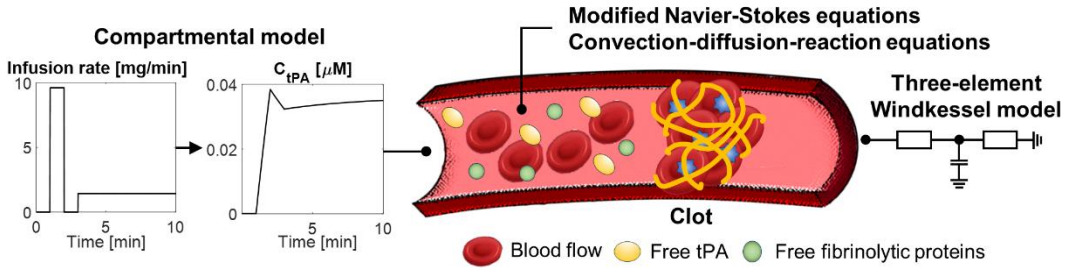

(a)

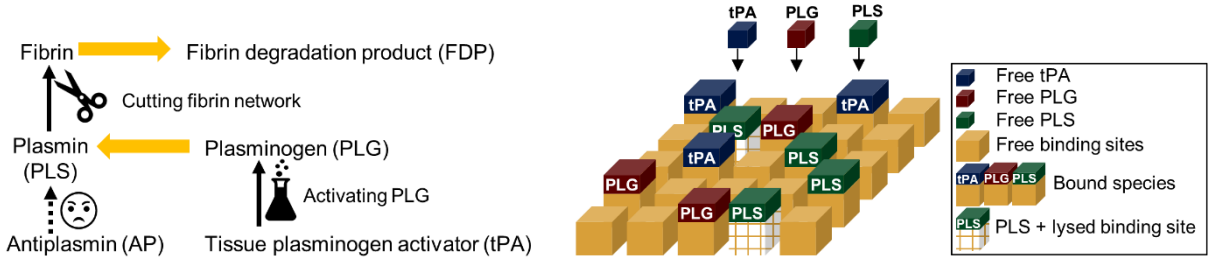

(b) (c)

Figure 1. A schematic illustration of the overall computational model. (a) Models for blood flow and species transport coupled with the compartmental model and three-element Windkessel model at the inlet and outlet boundaries, respectively. (b) Fibrinolytic reactions involving tPA, plasminogen (PLG), plasmin (PLS) and anti-plasmin (AP). (c) Adsorption and desorption of tPA, PLG and PLS onto and from the binding sites in the fibrin fibre network in a clot.

2.2 Simulation scenarios

2.2.1 3D patient-specific arterial geometry

A 3D patient-specific geometry is reconstructed from 3D rotational angiography images using Mimics 19.0 (Materialise, Leuven). Formal ethics approval is not required for the use of these images which were anonymised prior to analysis. Figure 2 displays the front, side and top views (on the right, top left and bottom left, respectively) of the reconstructed geometry.

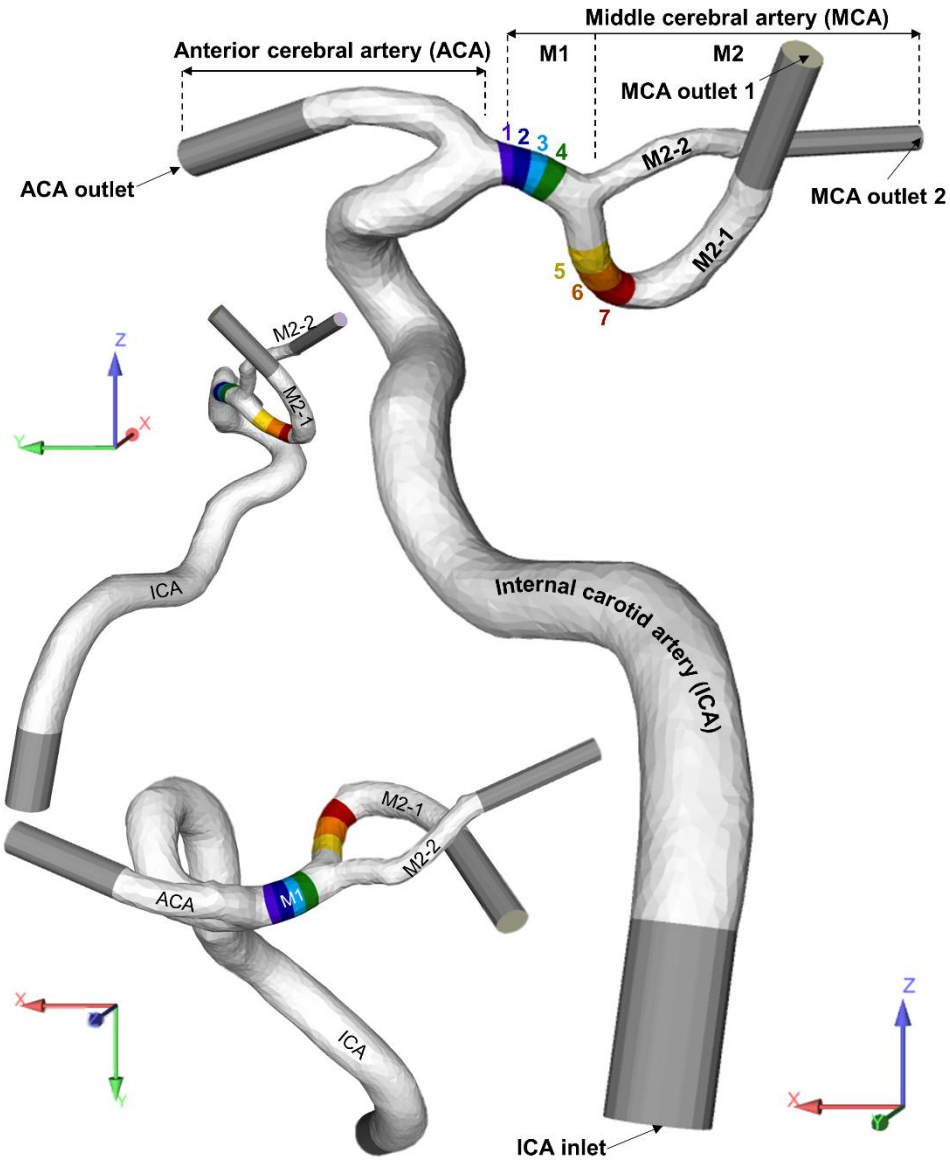

Figure 2. The patient-specific model used in this study. The internal carotid artery (ICA) bifurcates into ACA and MCA (M1), with the M1 segment of MCA bifurcating further into the inferior (M2-1) and superior (M2-2) branches. The coloured areas in the MCA represent the locations of clots. The grey parts are artificial extensions to the inlet and outlets.

As shown in Figure 2, clot regions are artificially assigned in the M1 segment and the M2 inferior branch (M2-1), respectively, based on clinical observations [23]. The volume of clot is varied from 4.6 to 24 mm^3 for M1 occlusion and from 9.6 mm^3 to 27 mm^3 for M2 occlusion in order to confine the obstructive

clot to the affected segment only. The clot volumes in our simulations are at the lower end of the range reported in a clinical study (mean volume of 129±120 mm^3 for ICA, M1 and M2 occlusions) [26], because the M1 segment of our patient-specific geometry is relatively short. The coloured areas numbered from 1 to 7 in Figure 2 represent different clot sizes, with the front and rear faces of each clot being perpendicular to the local centreline. Starting with the smallest clot, corresponding to region 1 and 5 for M1 and M2 occlusions respectively, different clot sizes are simulated by adding the subsequent clot regions one by one. Therefore a total of 7 scenarios are created, with clot volume varying from 1 to (1-4) for M1 occlusions and from 5 to (5-7) for M2 occlusions. Further geometric details of the model can be found in Supporting Information A.

2.2.2 Simulation and computational details

Blood flow is assumed to be Newtonian and laminar. Kinetics parameters for the fibrinolytic reactions and transport parameters are taken from our previous study, while the radius of fibrin fibre is chosen to be 65 nm [19]. The standard dosing protocol for the treatment of acute ischaemic stroke is used with a high dose 1.2 mg/kg in order to accelerate clot lysis for fast computation. The model equations are implemented in open source computational fluid dynamics (CFD) code, OpenFOAM 4.0, which utilises a finite volume spatial discretisation. The compartmental model is solved in MATLAB R2017a and the results are imported in the CFD code to serve as inlet conditions for the species transport model. Further computational details and simulation conditions are included in Supporting Information (Section B).

3. Simulation results

Here we present results for the 7 simulated scenarios with different occlusion sites and clot sizes. Each case is named based on the number of clots included in the simulation, as displayed in Figure 2. For example, the smallest and largest clots in the simulated M1 occlusions are referred to as C1 and C1-4, respectively; whereas those for M2 occlusions are C5 and C5-7, respectively.

3.1 Flow and clot lysis patterns for the largest clots at each occlusion site

First of all, flow patterns obtained from the simulations are analysed along with clot lysis patterns. Two scenarios with the largest clot at each occlusion site are selected for visualisation of flow and lysis patterns at representative time points.

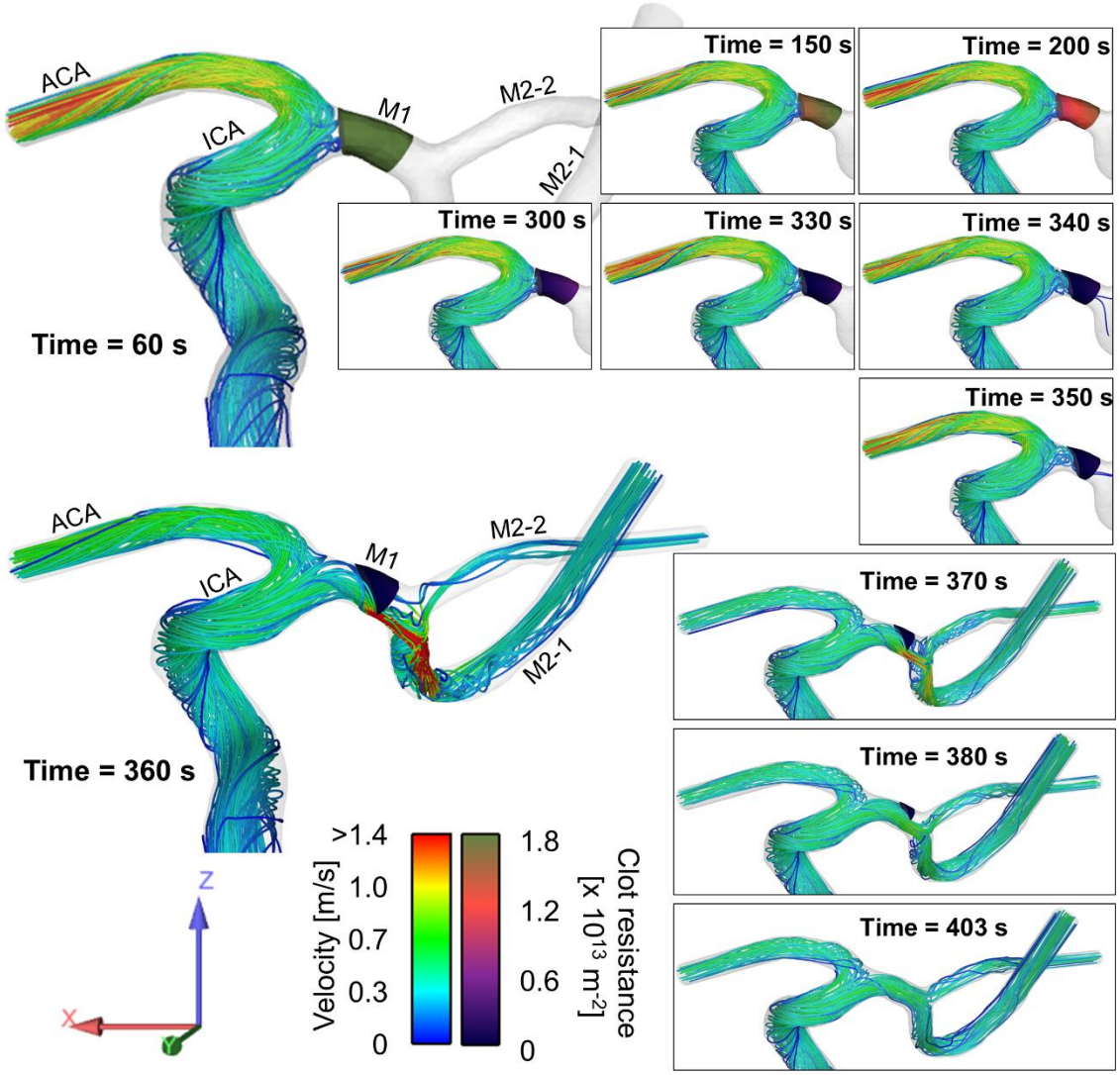

Figure 3. Flow and clot lysis patterns for C1-4 at different time points, from 60 (when the bolus infusion starts) to 403 seconds (when the clot completely disappears). Flow velocity and clot resistance (the inverse of clot permeability) are also colour coded.

Figure 3 shows changes in flow velocity and clot resistance for C1-4 from the start of bolus infusion (Time = 60 s) to complete lysis (Time = 403 s). Since the occluding clot, approximately 24 mm^3 in volume, is located in the M1 segment of MCA and very close to the ICA bifurcation, there is initially no visible flow in the M1 and M2 segments, with high clot resistance of 1.8×10^{13} m^{-2} (equivalent to permeability of 5.6×10^{-14} m^2), as can be seen at Time = 60 s in Figure 3. Relatively high flow velocities of up to 1.4 m/s can be seen at the ACA outlet as all the flow is directed to the ACA from the ICA. As a sufficient amount of tPA reaches the clot front, the clot starts to degrade from its front, leading to reduced clot resistance and increased permeability. The clot resistance gradually decreases from the time point of 150 to 300 s, with the clot volume starting to shrink at Time = 330 s. Due to the wide branching angle of the MCA, a recirculation zone is formed near the lower part of the M1 arterial wall, as can be seen at Time = 330, 340 and 350 s. This leads to faster clot dissolution around these areas due to the higher tPA concentration there and its faster penetration into the clot with reduced resistance, as evidenced by the spatial distribution of tPA within a clot in our previous work [19].

When the clot is sufficiently degraded with a substantial increase in its permeability, a little amount of flow starts to seep through, with a flow rate of 0.067 mL/s at Time = 350 s in the MCA. At around 360 seconds, a breakthrough path is established in the lower part of the clot, resulting in a high-velocity jet with a velocity magnitude of > 4 m/s. After the breakthrough, convective transport of tPA becomes dominant, transiently accelerating clot lysis. A small portion of clot remains attached to the upper wall of MCA until it is completely dissolved at 403 seconds.

For the M2 occlusion scenario of C5-7 shown in Figure 4, the inlet flow splits into two streams in the ACA and M2-2 owing to the blockage in the M2-1 at Time = 60 s. It is noticed that flow velocity in the ACA is lower in this scenario than that in Figure 3. Since the clot is located slightly distal to the M1 bifurcation, there is a large stagnation zone between the M1 bifurcation and the clot front in the M2-1. This results in a slower degradation of C5-7 than C1-4. The clot becomes smaller by gradual dissolution

from its front after Time = 300 seconds. When sufficient tPA permeates through the clot, more flow is seen to pass through, i.e., M2-1 flow rate of 0.0025 and 0.068 mL/s at Time = 450 s and 457 s, respectively.

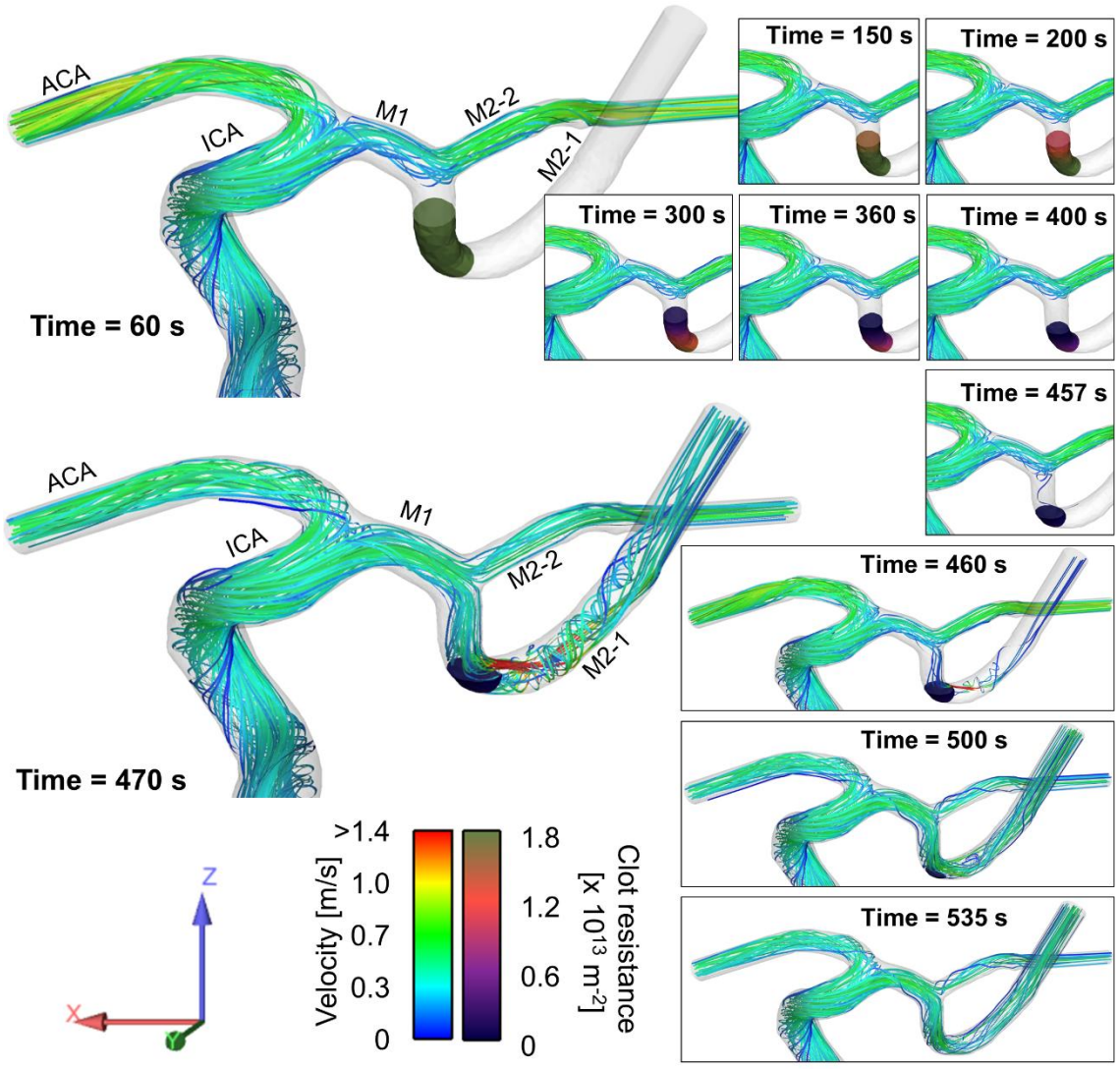

Figure 4. Flow and clot lysis patterns for C5-7 at different time points, from 60 (when the bolus infusion starts) to 535 seconds (when clot completely disappears). Flow velocity and clot resistance (the inverse of clot permeability) are also colour coded.

Lysis patterns are rather flat before Time = 400 s due to the M2-1 segment originating almost vertically from the M1 bifurcation. Afterwards, however, the clot front becomes highly skewed with the part near the inner curvature dissolving much faster than that near the outer curvature, resulting clot breakthrough at the inner curvature, shown at Time = 460 s. The high-velocity jet is also observed in the breakthrough pathway, with a maximum velocity of 4.2 m/s. This enables faster transport of tPA to the M2-1 and consequently increases the rate of clot lysis. Due to the high flow velocity in the presence of partially dissolving clot, the flow is highly disturbed and helical, as can be seen at Time = 470 s. The clot volume rapidly decreases after the breakthrough, although the reduction in clot volume slows down slightly, as noticed at Time = 470 to 535 s. This is attributed to the high degree of curvature where the remaining clot is located.

3.2 Flow rate and pressure variations over time

Figure 5 displays flow rates and pressures over time at the ICA, ACA, M2-1 and M2-2 for C1-4 and C5-7. For C1-4, flow rates at both M2 branches, M2-1 and M2-2, are initially zero and then restore to 1.76 mL/s and 0.79 mL/s, respectively, at 6.4 minutes (i.e., 5.4 minutes after the start of tPA injection at 1 min), as can be seen in Figures 5 (a) and (b). To avoid confusion, times that are referred to in this section and hereafter represent the simulation time inclusive of an initial 1 minute of flow stabilisation without tPA injection, unless otherwise stated. Pressures in the M2-1 and M2-2 follow a similar pattern, which are initially zero when there is no flow and rise to 60 mmHg after recanalization.

For C5-7 where only M2-1 is blocked, the ICA flow is initially divided into the M2-2 and ACA branches at 1.35 and 2.96 mL/s, respectively. Once the breakthrough path is made at 8.7 minutes, the flow in the M2-1 is fully restored to 1.76 mL/s whereas M2-2 and ACA flow rates drop to 0.80 and 1.75 mL/s, respectively. As shown in Figures 5 (b) and (c), pressures at the M2-2 and ACA outlet before the breakthrough are 100.3 and 102.2 mmHg, respectively, which fall back to 60 mmHg after breakthrough. Interestingly, initial pressures at the ICA inlet are calculated to be 160 and 110 mmHg for C1-4 and C5-7,

respectively, as depicted in Figure 5 (d), possibly due to the assumption of same inflow for the two types of occlusion.

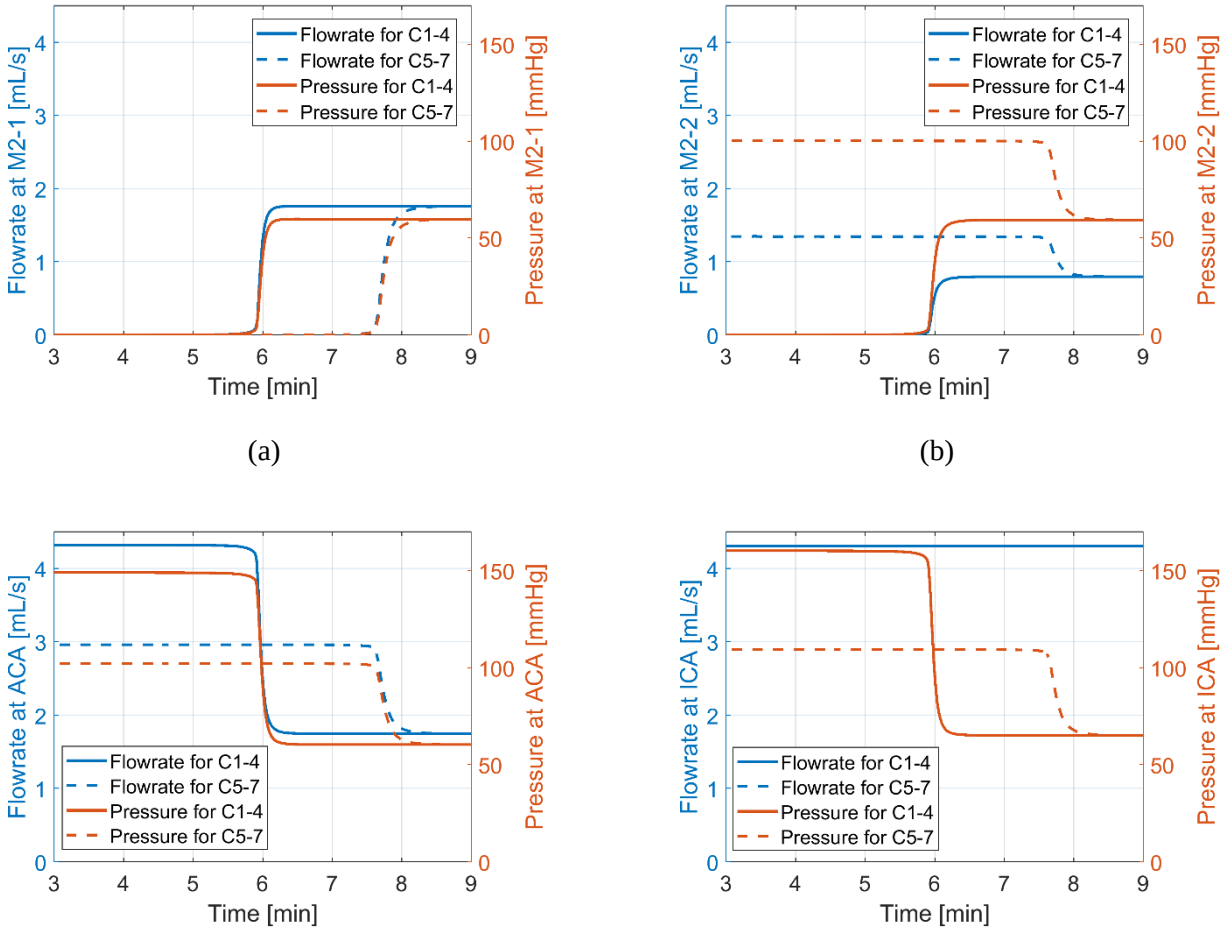

Figure 5. Flow rate and pressure variations over time for the largest clots of each occlusion. Flow rate and pressure at (a) M2-1 outlet (occluding branch for C5-7), (b) M2-2 outlet, (c) ACA outlet and (d) ICA inlet. The solid and dashed lines are results of C1-4 (M1 occlusion) and C5-7 (M2 occlusion), respectively. Blue coloured lines are for flow rate and orange coloured lines for pressure. The *x*-axis denotes the simulation time, inclusive of an initial 1 minute of flow stabilisation without tPA injection. This applies to all subsequent figures unless otherwise stated.

In order to compare the breakthrough times of all scenarios studied here, ACA flow rates over time are displayed in Figure 6 along with the initial clot volumes. The M1 occlusions achieve the breakthrough of clots at around 5.6 to 6.5 min, while the M2 occlusions take between 6 to 8.7 min, as shown in Figure 6 (a). It can also be observed that the ACA flow rates slowly decrease before breakthrough due to an increasing degree of clot degradation and clot permeability, which allows some flow to pass through the clot, as observed in Figures 3 and 4.

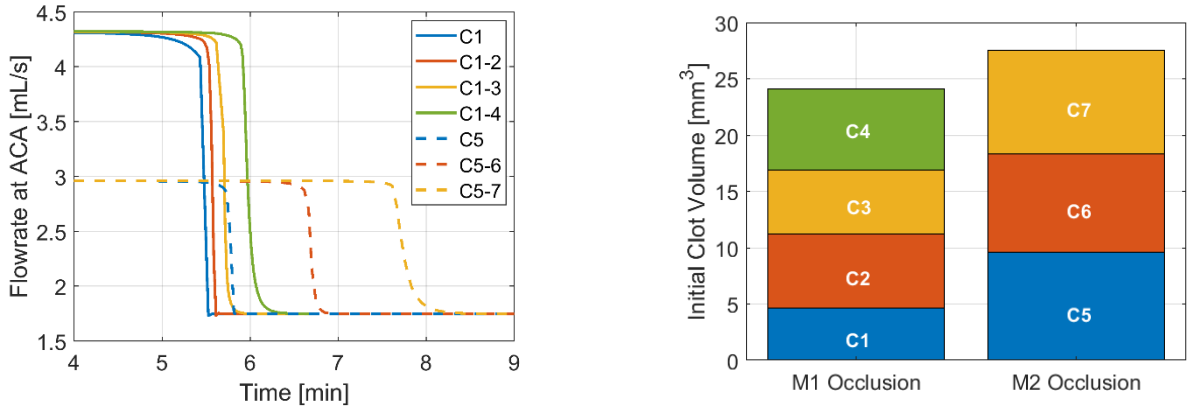

(a) (b)

Figure 6. Flow rate variations in ACA outlet over time for all cases. (a) ACA flow rates and (b) initial clot volumes.

For clots of a similar size but at different locations, clots in M2 occlusions tend to dissolve slowly than those in M1 occlusions. For example, C1-2 dissolves faster than C5 although the volume of C1-2 (11.3 mm^3) is about 1.1 times larger than that of C5 (9.58 mm^3). The discrepancy between two occlusion sites becomes more prominent as the clot size is increased, e.g., breakthrough times of C1-4 and C5-7 differ by 2.3 min. This could be attributed to differences in the geometric features of patient-specific vasculature and the position of clot front from each bifurcation.

3.3 Concentrations of free and bound tPA within the clot

Figure 7 shows free and bound tPA concentrations within the remaining clot. The free tPA concentration increases rapidly after the bolus injection at 1 min, as seen in Figure 7 (a). For all the scenarios except for C5-7, free tPA concentration peaks at between 2 and 3 minutes. This is due to the rapid increase in the level of tPA in the plasma after the initial bolus injection, as can be seen in Figure 1 (a) and in our previous work [19]. It is also noticed that the concentration peaks for C1-3 and C5 almost overlap even though C1-3 is about 1.8 times larger than C5. This is because C5 is located more distally, meaning that tPA transport in the M2 occlusion is initially driven by diffusion. Once the bolus injection is completed at 2 min, free tPA concentration within the clot falls slightly due to a delayed start of continuous infusion. Thereafter, the continuous infusion keeps the level of tPA high in the clot (above 0.03 μM) as well as in the plasma. In addition, it can be observed that the concentration peak at the end of bolus injection becomes less distinct and eventually disappears as the clot becomes larger, as in C5-7.

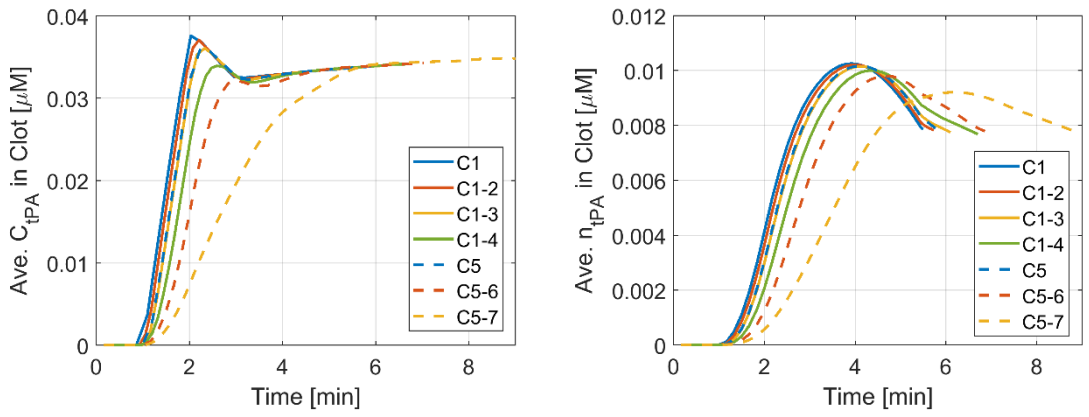

(a) (b)

Figure 7. Volume-averaged concentrations of (a) free tPA and (b) bound tPA within each clot.

The concentration of bound tPA in the clot, on the other hand, seems to be less affected by the bolus injection of tPA and time delay between two infusion modes, as displayed in Figure 7 (b). The bound tPA smoothly increases from 1 min and continues to rise even during the delay interval, and then eventually falls off. Peaks of bound tPA concentration lag slightly behind those of free tPA. Moreover, the

maximum concentration of bound tPA in each clot is much lower than that of free tPA, at a maximum of between 0.009 and 0.01 μM. In all scenarios, the bound tPA concentration falls to around 0.008 μM before complete lysis is achieved.

3.4 Clot volume and lysis completion time

Finally, the progression of clot lysis is examined by monitoring changes in clot volume over time, as shown in Figure 8 (a). Despite the different locations of the clots between the M1 and M2 occlusions, they all start to decrease in size at around 5.4 minutes. The trend of reduction in clot volume is almost linear, while the rate of reduction slows down as approaching the completion of lysis.

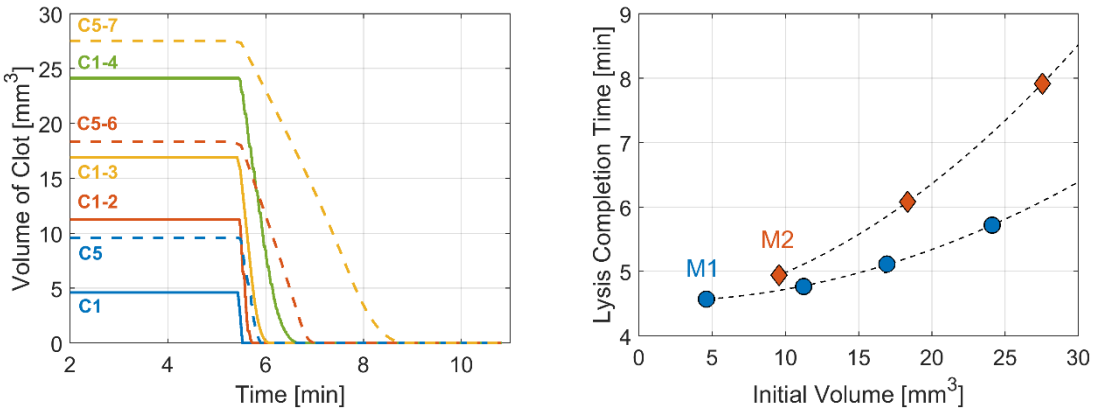

(a) (b)

Figure 8. Clot volume and lysis completion time. (a) Change in the volume of clot over time and (b) the lysis completion times from the start of bolus injection as a function of initial clot volume for each occlusion site. The black dashed lines are obtained by quadratic interpolation of simulation results for each occlusion.

For each occlusion site, complete lysis is achieved earlier for smaller initial clot volumes, as expected, at 5.6 to 6.1 mins for C1 to C1-4 and 5.9 to 8.9 min for C5 to C5-7. However, when comparing different locations for similarly sized clots, M2 occlusions take longer for complete lysis than M1 occlusions, e.g.,

C1-2 vs C5 and C1-3 vs C5-6. This is more evident when examining the lysis completion time (i.e., the time when clot volume becomes zero–1 min, as the bolus is injected at 1 min) as a function of initial clot volume for each occlusion site, displayed in Figure 8 (b) where the simulation results (symbols) and fitted curves (black dashed lines) are shown. Lysis completion times for both occlusions exhibit approximately a quadratic increase with respect to the initial volume of clots, although the M1 occlusions are less sensitive to the size of clot than the M2 occlusions. Based on the simulation results, it can be said that M2 clots take a longer time to completely dissolve than M1 clots for the same size. It is also expected that differences in lysis completion time between the two occlusions would increase as the clot becomes larger.

4. Discussions and conclusions

First of all, flow and lysis patterns in scenarios with the largest clot in the M1 and M2 segments are visualised at several time points and further analysed with respect to flow velocity and clot resistance. In both clots, an asymmetric lysis front is formed; faster lysis takes place in the inner curvature of the arterial walls than in the outer curvature. As a result, a breakthrough pathway is always established from the clot region adjacent to the inner curvature, as seen in Figures 3 and 4. Since the clot fronts are perpendicular to their local centreline, initial volume reduction is also observed at the inner curvature due to the presence of recirculation and consequently prolonged residence time of tPA in that region. This can be corroborated by the spatial distributions of fibrinolytic proteins and the extent of lysis within the clot, presented in our previous study [19]. Even when the clot front is not normal to the centreline, the trend of the breakthrough path being developed near the inner curvature is expected to be preserved with a slight variation in the initial lysis pattern.

It is also worth pointing out that clot lysis slows down as the clot front becomes aligned almost parallel to the flow direction. This indicates that intravenous infusion of tPA may be ineffective at this stage, which can also occur in scenarios where non-occlusive clots are present, which partially block the arteries and allow blood flow to pass through at higher velocities. Furthermore, there is a high chance of clot

deformation and even embolisation due to high shear rates in the partially blocked vessels, which may lead to secondary blockages in small blood vessels [28–30]. Therefore, alternative technologies might be needed in order to improve the effectiveness of thrombolytic therapy.

In addition, flow rate and pressure in each arterial branch are obtained from the simulations and compared between the largest clots in the M1 and M2 occlusions. After flow is restored in an occluded branch, both cases achieve the same flow split: 1.75 and 2.56 mL/s for ACA and MCA, respectively. These values are slightly larger than those reported in the literature [31,32] but thought to be reasonable, given that there are large individual variations of average ICA flow rate, from 3.4 mL/s to 5.4 mL/s [33]. Pressure differences between the ICA and M2-1 are calculated to be approximately 160 and 100 mmHg for M1 and M2 occlusions, respectively. These seem to be within the range expected for occlusive clots, based on results of the existing computational study where the circle of Willis and its variations were simulated in the presence of up to 96% carotid stenosis [34]; approximately 100 mmHg could be expected for 100% stenosis by extrapolating their data. It is also worth mentioning that calculated ICA pressures for M1 and M2 occlusions before recanalisation differ by 60 mmHg, as shown in Figure 5 (d). This is due to the assumption of same ICA flow rate in both scenarios, which might not be realistic. It has been shown that flow distribution could be altered if there are anatomical variations or vessel occlusions in the circle of Willis when the same amount of blood flow is pumped from the heart [35]. It would therefore be necessary to apply patient-specific flow data at the inlet of ICA in order to gain more realistic pressure and flow rate at each outlet, which was not possible in this work due to the lack of patient data.

Breakthrough times are also identified for all scenarios based on temporal changes in ACA flow rate. Simulation results show that M2 occlusions tend to dissolve more slowly than M1 occlusions for the same clot size. This is mainly due to two reasons; first, the clots in the M2 segment are located more distally from the M1 bifurcation, so that majority of the tPA passing through the M1 segment is diverted to the patent M2-2 branch. As a result, it takes more time for a sufficient amount of tPA to reach the clot front

during the initial stage of the treatment. Second, the higher degree of arterial curvature in the M2 branch than in the M1 makes the clot lysis front parallel to the flow direction in the later stage of clot lysis, leading to rapid loss of tPA to the downstream circulation, as discussed above.

Concentrations of free and bound tPA in a clot, on the other hand, are more related to the tPA dosage regimen and resulting level of tPA in the plasma. As discussed in the previous study [19], free tPA level in the plasma rapidly increases by the initial bolus injection and then plummet due to the time delay before the continuous infusion. This dynamic change of the plasma tPA is partly mirrored in the concentration of free phase tPA delivered to the clot, while the largest clot in the M2 does not show any sign of influence by the initially elevated tPA concentration in the plasma. This suggests that occlusions with a long clot might not benefit from the bolus injection that aims to rapidly raise the tPA concentration, as concluded for fine clots in the previous study [19]. In addition, the concentration peaks of free tPA in the M2 appears slightly later than in the M1 when the clot sizes are similar, due to the distal location of the M2 clots. This implies that the distance between the bifurcation and clot front is an important factor in determining the initial transport rate of tPA to the clot.

It can also be observed that the concentration of bound tPA is approximately 3.5 times lower than that of free tPA. This could be for two reasons: competition among the fibrinolytic proteins for binding with the fibrin fibre and limited adsorption rate of tPA itself. Our computer model might therefore be advantageous in testing different tPA drugs with higher fibrin specificity or new nanomedicines that better target the clot in order to investigate their potential as an alternative method.

Finally, simulation results are analysed in terms of changes in clot volume over time and lysis completion times against the initial volume of clots in each location. All clots achieve recanalisation within 8 minutes from the start of the treatment. As addressed in the previous study, our model describes the clot as a fibrin fibre network of higher permeability than a real clot with cellular components lodged within the fibre

network. Moreover, a higher tPA dose, 1.2 mg/kg, is used in our simulations compared to tPA doses used in clinical studies (0.9 mg/kg or 0.6 mg/kg) [36–38]. These assumptions lead to accelerated tPA transport through the clot, hence faster recanalisation than clinical observations; mean recanalisation durations of 23±16 min [38] and 47±32 min [37] in two separate studies of tPA-treated stroke patients where recanalisation was monitored via transcranial Doppler (TCD). Also, Christou et al. [36] correlated recanalisation timings measured through TCD with clinical outcomes in stroke patients, and they found that 50% of all studied patients achieved complete or partial recanalisation within 31-60 min after tPA bolus and 25% of them within 0-30 min. Additionally, the clot sizes adopted in our simulations are relatively small. Riedel et al. reported that clot lengths exceeding 8 mm are likely to fail in recanalisation for acute MCA stroke [25], while Yoo et al. estimated a cut-off value for non-recanalisation to be 200 mm^3 based on a study of 214 patients with acute ischaemic stroke [26]. The largest clot in our simulation is approximately 5.7 mm in length and 27 mm^3 in volume, much smaller than the reported threshold values. Furthermore, it is worth noting that there appears to be a contradiction between our simulation results and clinical observations: our model predicts that M2 occlusions need a longer time to achieve recanalisation than M1 occlusions, whereas clinical studies reported that patients with distal occlusion were more likely to have successful recanalisation and a good outcome than those with proximal occlusion [22,23,27]. However, an important difference is that in clinical studies distal clots are usually smaller than proximal clots [21,22], whereas the same clot size is assumed in our simulations when comparing M1 and M2 occlusions.

In conclusion, our simulation results for various clot sizes at two locations support clinical observations that clot size has a strong influence on recanalisation success and lysis time. Our results further reveal that: (i) arterial curvature is an important factor in determining lysis and breakthrough patterns, (ii) clot location affects the rate of tPA accumulation at the clot front and the initial lysis rate, and (iii) arterial curvature also influences the late-stage lysis rate, especially after breakthrough. This study demonstrates that our simulation platform for thrombolysis in ischaemic stroke can offer an in-depth understanding of

406 drug transport and clot lysis under various clinical scenarios where numerous parameters are involved,
407 such as the clot location and size studied here as well as clot permeability and drug dose as addressed in
408 our previous study. Furthermore, the model can potentially be used to help with benefit/risk calculations
409 based on clot size and location obtained from patient scans. This would help determine which patient is
410 more likely to achieve successful recanalisation with intravenous thrombolysis within a limited time
411 window. In the future, we hope to further improve the model by incorporating the presence of cellular
412 components in the clot, and to extend the model to simulate new tPA delivery systems for targeted
413 thrombolytic therapy. The model can be further improved by applying more realistic haemodynamic
414 conditions, e.g. physiological pulsatile flow at the inlet instead of a steady flow rate in order to capture
415 detailed lysis patterns influenced by flow pulsatility and mixing effects near the lysis front. In addition,
416 the potential effect of turbulence on drug transport and lysis rate is worth investigating, as the high-
417 velocity jet observed during the clot breakthrough could induce transition to turbulence which may affect
418 local flow and lysis patterns.
419
420
421 **Conflicts of interest**
422 None.
423
424 **Acknowledgements**
425 This research was supported by the National Institute for Health Research (NIHR) Biomedical Research
426 Centre based at Imperial College Healthcare NHS Trust and Imperial College London. The views
427 expressed are those of the authors and not necessarily those of the NHS, the NIHR or the Department of
428 Health. ADH receives support from the British Heart Foundation (PG/15/75/31748, CS/15/6/31468,
429 CS/13/1/30327), the National Institute for Health Research University College London Hospitals
430 Biomedical Research Centre and works in a unit that receives support from the UK Medical Research
431 Council (Programme Code MC_UU_12019/1).

Ethical approval

Not required.

Data statement

Data are available from the corresponding author on request.

References

[1] Durukan A, Tatlisumak T. Acute ischemic stroke: Overview of major experimental rodent models, pathophysiology, and therapy of focal cerebral ischemia. Pharmacol Biochem Behav 2007;87:179–97. doi:10.1016/j.pbb.2007.04.015.

[2] Bivard A, Lin L, Parsonsb MW. Review of Stroke Thrombolytics. J Stroke 2013;15:90. doi:10.5853/jos.2013.15.2.90.

[3] Moussaddy A, Demchuk AM, Hill MD. Thrombolytic therapies for ischemic stroke: Triumphs and future challenges. Neuropharmacology 2018;134:272–9. doi:10.1016/j.neuropharm.2017.11.010.

[4] Adeoye O, Hornung R, Khatri P, Kleindorfer D. Recombinant tissue-type plasminogen activator use for ischemic stroke in the united states: A doubling of treatment rates over the course of 5 years. Stroke 2011. doi:10.1161/STROKEAHA.110.612358.

[5] Kucinski T, Koch C, Eckert B, Becker V, Krömer H, Heesen C, et al. Collateral circulation is an independent radiological predictor of outcome after thrombolysis in acute ischaemic stroke. Neuroradiology 2003;45:11–8. doi:10.1007/s00234-002-0881-0.

[6] Wufuer A, Wubuli A, Mijiti P, Zhou J, Tuerxun S, Cai J, et al. Impact of collateral circulation status on favorable outcomes in thrombolysis treatment: A systematic review and meta-analysis. Exp Ther Med 2018;15:707–18. doi:10.3892/etm.2017.5486.

[7] Hong K-S, Ko S-B, Lee JS, Yu K-H, Rha J-H. Endovascular Recanalization Therapy in Acute Ischemic Stroke: Updated Meta-analysis of Randomized Controlled Trials. J Stroke 2015;17:268–

81. doi:10.5853/jos.2015.17.3.268.

[8] Scheitz JF, Abdul-Rahim AH, Macisaac RL, Cooray C, Sucharew H, Kleindorfer D, et al. Clinical Selection Strategies to Identify Ischemic Stroke Patients with Large Anterior Vessel Occlusion: Results from SITS-ISTR (Safe Implementation of Thrombolysis in Stroke International Stroke Thrombolysis Registry). Stroke 2017;48:290–7. doi:10.1161/STROKEAHA.116.014431.

[9] Behme D, Kowoll A, Weber W, Mpotsaris A. M1 is not M1 in ischemic stroke: The disability-free survival after mechanical thrombectomy differs significantly between proximal and distal occlusions of the middle cerebral artery M1 segment. J Neurointerv Surg 2015;7:559–63. doi:10.1136/neurintsurg-2014-011212.

[10] Evans MRB, White P, Cowley P, Werring DJ. Revolution in acute ischaemic stroke care: A practical guide to mechanical thrombectomy. Pract Neurol 2017;17:252–65. doi:10.1136/practneurol-2017-001685.

[11] Pfaff J, Herweh C, Pham M, Schieber S, Ringleb PA, Bendszus M, et al. Mechanical thrombectomy of distal occlusions in the anterior cerebral artery: Recanalization rates, periprocedural complications, and clinical outcome. Am J Neuroradiol 2016;37:673–8. doi:10.3174/ajnr.A4594.

[12] Grossberg JA, Rebello LC, Haussen DC, Bouslama M, Bowen M, Barreira CM, et al. Beyond Large Vessel Occlusion Strokes: Distal Occlusion Thrombectomy. Stroke 2018;49:1662–8. doi:10.1161/STROKEAHA.118.020567.

[13] Kurre W, Aguilar-Pérez M, Martinez-Moreno R, Schmid E, Bäzner H, Henkes H. Stent Retriever Thrombectomy of Small Caliber Intracranial Vessels Using pREset LITE: Safety and Efficacy. Clin Neuroradiol 2017;27:351–60. doi:10.1007/s00062-016-0497-0.

[14] Mistry EA, Mistry AM, Nakawah MO, Chitale R V., James RF, Volpi JJ, et al. Mechanical Thrombectomy Outcomes with and Without Intravenous Thrombolysis in Stroke Patients: A Meta-Analysis. Stroke 2017;48:2450–6. doi:10.1161/STROKEAHA.117.017320.

[15] Minnerup J, Wersching H, Teuber A, Wellmann J, Eyding J, Weber R, et al. Outcome after

Thrombectomy and Intravenous Thrombolysis in Patients with Acute Ischemic Stroke: A Prospective Observational Study. Stroke 2016;47:1584–92. doi:10.1161/STROKEAHA.116.012619.

[16] Campbell BCV, Mitchell PJ, Churilov L, Yassi N, Kleinig TJ, Yan B, et al. Tenecteplase versus alteplase before endovascular thrombectomy (EXTEND-IA TNK): A multicenter, randomized, controlled study. Int J Stroke 2018;13:328–34. doi:10.1177/1747493017733935.

[17] Campbell BCV, Mitchell PJ, Churilov L, Yassi N, Kleinig TJ, Dowling RJ, et al. Tenecteplase versus Alteplase before Thrombectomy for Ischemic Stroke. N Engl J Med 2018;378:1573–82. doi:10.1056/NEJMOA1716405.

[18] Piebalgs A, Xu XY. Towards a multi-physics modelling framework for thrombolysis under the influence of blood flow. J R Soc Interface 2015. doi:10.1098/rsif.2015.0949.

[19] Piebalgs A, Gu B, Roi D, Lobotesis K, Thom S, Xu XY. Computational Simulations of Thrombolytic Therapy in Acute Ischaemic Stroke. Sci Rep 2018;8:15810. doi:10.1038/s41598-018-34082-7.

[20] Yan S, Chen Q, Xu M, Sun J, Liebeskind DS, Lou M. Thrombus Length Estimation on Delayed Gadolinium-Enhanced T1. Stroke 2016. doi:10.1161/STROKEAHA.115.011401.

[21] Kamalian S, Morais LT, Pomerantz SR, Aceves M, Sit SP, Bose A, et al. Clot length distribution and predictors in anterior circulation stroke: Implications for intra-arterial therapy. Stroke 2013. doi:10.1161/STROKEAHA.113.003079.

[22] Friedrich B, Gawlitza M, Schob S, Hobohm C, Raviolo M, Hoffmann KT, et al. Distance to thrombus in acute middle cerebral artery occlusion: A predictor of outcome after intravenous thrombolysis for acute ischemic stroke. Stroke 2015. doi:10.1161/STROKEAHA.114.008454.

[23] Saqqur M, Uchino K, Demchuk AM, Molina CA, Garami Z, Calleja S, et al. Site of arterial occlusion identified by transcranial Doppler predicts the response to intravenous thrombolysis for stroke. Stroke 2007;38:948–54. doi:10.1161/01.STR.0000257304.21967.ba.

[24] Rohan V, Baxa J, Tupy R, Cerna L, Sevcik P, Friesl M, et al. Length of occlusion predicts

recanalization and outcome after intravenous thrombolysis in middle cerebral artery stroke. Stroke 2014;45:2010–7. doi:10.1161/STROKEAHA.114.005731.

[25] Riedel CH, Zimmermann P, Jensen-Kondering U, Stingele R, Deuschl G, Jansen O. The importance of size: Successful recanalization by intravenous thrombolysis in acute anterior stroke depends on thrombus length. Stroke 2011;42:1775–7. doi:10.1161/STROKEAHA.110.609693.

[26] Yoo J, Baek J-H, Park H, Song D, Kim K, Hwang IG, et al. Thrombus Volume as a Predictor of Nonrecanalization After Intravenous Thrombolysis in Acute Stroke. Stroke 2018;49:2108–15. doi:10.1161/STROKEAHA.118.021864.

[27] Saarinen JT, Sillanpää N, Rusanen H, Hakomäki J, Huhtala H, Lähteelä A, et al. The mid-M1 segment of the middle cerebral artery is a cutoff clot location for good outcome in intravenous thrombolysis. Eur J Neurol 2012;19:1121–7. doi:10.1111/j.1468-1331.2012.03689.x.

[28] Xu S, Xu Z, Kim O V., Litvinov RI, Weisel JW, Alber M. Model predictions of deformation, embolization and permeability of partially obstructive blood clots under variable shear flow. J R Soc Interface 2017;14. doi:10.1098/rsif.2017.0441.

[29] Kim O V., Liang X, Litvinov RI, Weisel JW, Alber MS, Purohit PK. Foam-like compression behavior of fibrin networks. Biomech Model Mechanobiol 2016. doi:10.1007/s10237-015-0683-z.

[30] Cines DB, Lebedeva T, Nagaswami C, Hayes V, Massefski W, Litvinov RI, et al. Clot contraction: Compression of erythrocytes into tightly packed polyhedra and redistribution of platelets and fibrin. Blood 2014. doi:10.1182/blood-2013-08-523860.

[31] Enzmann DR, Ross MR, Marks MP, Pelc NJ. Blood flow in major cerebral arteries measured by phase-contrast cine MR. Am J Neuroradiol 1994. doi:10.1007/978-3-642-79434-6_18.

[32] Stock KW, Wetzel SG, Lyrer PA, Radü EW. Quantification of blood flow in the middle cerebral artery with phase-contrast MR imaging. Eur Radiol 2000. doi:10.1007/s003300000378.

[33] Bogren HG, Buonocore MH, Gu W -Z. Carotid and vertebral artery blood flow in left- and right-handed healthy subjects measured with MR velocity mapping. J Magn Reson Imaging 1994. doi:10.1002/jmri.1880040110.

[34] Long Q, Luppi L, König CS, Rinaldo V, Das SK. Study of the collateral capacity of the circle of Willis of patients with severe carotid artery stenosis by 3D computational modeling. J Biomech 2008;41:2735–42. doi:10.1016/j.jbiomech.2008.06.006.

[35] Alastruey J, Parker KH, Peiró J, Byrd SM, Sherwin SJ. Modelling the circle of Willis to assess the effects of anatomical variations and occlusions on cerebral flows. J Biomech 2007;40:1794–805. doi:10.1016/j.jbiomech.2006.07.008.

[36] Christou I, Alexandrov AV, Burgin WS, Wojner AW, Felberg RA, Malkoff M. Timing of recanalization after tissue plasminogen activator therapy determined by transcranial Doppler correlates with clinical recovery from ischemic stroke. Stroke 2000;31:1812–6.

[37] Molina CA, Ribo M, Rubiera M, Montaner J, Santamarina E, Delgado-Mederos R, et al. Microbubble administration accelerates clot lysis during continuous 2-MHz ultrasound monitoring in stroke patients treated with intravenous tissue plasminogen activator. Stroke 2006;37:425–9. doi:10.1161/01.STR.0000199064.94588.39.

[38] Alexandrov A V, Burgin WS, Demchuk AM, El-mitwalli A, Grotta C. Speed of Intracranial Clot Lysis With Intravenous Tissue. Circulation 2001;103:2897–902.

Supporting Information

Computational Simulations of Thrombolysis in Acute Stroke: Effect of Clot Size and Location on Recanalisation

Boram Gu[1], Andris Piebalgs[1], Yu Huang[1], Dylan Roi[2], Kyriakos Lobotesis[2], Colin Longstaff[3], Alun D. Hughes[4,5], Rongjun Chen[1], Simon A. Thom[6], Xiao Yun Xu[1,*]

[1]Department of Chemical Engineering, Imperial College London, South Kensington Campus, London, United Kingdom

[2]Imaging Department, Charing Cross Hospital, Imperial College Healthcare NHS Trust, London W6 8RF, United Kingdom

[3]Biotherapeutics Section, National Institute for Biological Standards and Control, South Mimms, Herts, United Kingdom

[4]Institute of Cardiovascular Science, University College London, London, United Kingdom

[5]MRC Unit for Lifelong Health and Ageing at University College London, London, United Kingdom

[6]National Heart & Lung Institute, Imperial College London, Hammersmith Campus, London, United Kingdom

*Corresponding author. Email address: yun.xu@imperial.ac.uk (X.Y. Xu)

A. Further geometric details

It consists of an ICA that bifurcates into the A1 segment of ACA and the M1 segment of MCA that further bifurcates into the superior and inferior branches, namely M2-2 and M2-1, respectively. Suitable extensions are added to the inlet of ICA and exits of the three cerebral branches, coloured in grey, to allow for flow development and ensure numerical stability. The selection of clot size is limited by the dimensions of the patient-specific arterial geometry used in this study; the M1 segment is relatively short at 7.24 mm compared to a reported average length of 9.4 mm with a range of 4.3 to 19.5 mm [1], and the maximum size of M2 clot is adjusted to be comparable to that of the M1 clot. Geometric details are listed in Table A.1 where the length of each branch is measured along the vessel centreline.

587 Table A.1. Geometrical parameters

Description	Value [mm or mm^3]
Diameter of ICA inlet	5.59
Diameter of ACA outlet	2.52
Diameter of M2-1 outlet	2.55
Diameter of M2-2 outlet	1.73
Mean diameter of clots in M1	3.07
Mean diameter of clots in M2-1	2.48
Length of ICA	79.2
Length of ICA extension	10.0
Length of ACA	12.1
Length of ACA extension	10.0
Length of M1	7.24
Length of M2-1	22.2
Length of M2-1 extension	9.55
Length of M2-2	16.4
Length of M2-2 extension	9.78
Volume of Clot 1	4.61
Volume of Clot 1-2	11.3
Volume of Clot 1-3	16.9
Volume of Clot 1-4	24.1
Volume of Clot 5	9.58
Volume of Clot 5-6	18.4
Volume of Clot 5-7	27.5

588

589 **B. Computational Details**

590 **B.1 Model parameters and simulation conditions**

591 Blood flow is assumed to be Newtonian and laminar. Kinetics parameters for the fibrinolytic reactions
592 and transport parameters are taken from our previous study, while the radius of fibrin fibre is chosen to be
593 65 nm [2]. A steady flow rate of 4.31 mL/s is imposed at the ICA inlet, which is obtained by averaging
594 the pulsatile flow rate over a cycle found in the literature [3]. No-slip conditions and rigid wall are
595 specified at all parts of arterial walls. The three-element Windkessel model is adopted as the outflow
596 boundary condition at all outlets, with its parameters being calculated based on flow distributions
597 proportional to the cross-sectional areas of each outlet [4] and an outlet pressure of 60 mmHg [5,6], in the

absence of patient-specific flow and pressure measurements. The derived parameter values are listed in Table B.1. For the species transport equations, time-varying concentrations of tPA, PLG, PLS and AP calculated from the compartmental model are provided to the 3D model to serve as its inlet boundary condition. The recommended dosage regimen for the treatment of acute ischaemic stroke is intravenous (IV) administration of 0.9 mg of tPA/kg of patient weight with 10% of the total dose administered as an initial bolus over 1 minute and the remaining 90% infused over an hour [7]. It was found in our previous study that higher tPA doses would accelerate clot lysis without affecting lysis patterns [2]. Since simulations to capture the progression of clot lysis until complete dissolution are computationally intensive, a high dose 1.2 mg/kg with a patient weight of 80 kg is chosen for simulations in this study. It is also assumed that there is a short delay of 1 minute between the bolus and continuous infusion. The concentration of tPA obtained from the compartmental model for the first 10 minutes is included in Figure 1, along with the infusion rate. Temporal concentrations of other proteins can be found in the previous work [2].

Table B.1Three-element Windkessel model parameters

Outlet	Description	Symbol	Value	Unit
ACA	Total resistance	$R_{t,ACA}$	4.61×10^{9}	$Pa\cdot s/m^3$
	Proximal resistance	$R_{p,ACA}$	2.17×10^{9}	$Pa\cdot s/m^3$
	Distal resistance	$R_{d,ACA}$	2.44×10^{9}	$Pa\cdot s/m^3$
	Capacitance	C_{ACA}	3.88×10^{-10}	m^3/Pa
MCA 1	Total resistance	$R_{T,MCA-1}$	4.53×10^{9}	$Pa\cdot s/m^3$
	Proximal resistance	$R_{p,ACA}$	2.13×10^{9}	$Pa\cdot s/m^3$
	Distal resistance	$R_{d,ACA}$	2.40×10^{9}	$Pa\cdot s/m^3$
	Capacitance	C_{MCA-1}	3.95×10^{-10}	m^3/Pa
MCA 2	Total resistance	$R_{T,MCA-2}$	9.87×10^{9}	$Pa\cdot s/m^3$
	Proximal resistance	$R_{p,ACA}$	5.17×10^{9}	$Pa\cdot s/m^3$
	Distal resistance	$R_{d,ACA}$	4.70×10^{9}	$Pa\cdot s/m^3$
	Capacitance	C_{MCA-2}	1.81×10^{-10}	m^3/Pa

B.2 Computational details

The model equations for blood flow and species transport are implemented in open source computational fluid dynamics (CFD) code, OpenFOAM 4.0, which utilises a finite volume spatial discretisation. The PIMPLE algorithm is employed for pressure-velocity coupling with a tolerance of 10^{-5} and 5×10^{-5} for

velocity and pressure, respectively. A blending function of Euler and Crank-Nicolson schemes is chosen for temporal integration with a blending coefficient of 0.9, recommended to ensure accuracy and robustness in OpenFOAM. A time step of 0.005 seconds and maximum iteration of 500 are used to ensure robust convergence and solution accuracy. The compartmental model is solved using an inbuilt ordinary differential equations solver in MATLAB, which is based on the Runge-Kutta method.

A computational mesh containing approximately 2 million hexahedral elements for the reconstructed geometry is created in ICEM CFD 15.0. This mesh is deemed sufficient following a mesh independence study with two additional meshes, consisting of around 0.9 million and 1.5 million elements, for the case of clot No. 1. Differences in lysis completion time are less than 4 seconds and calculated ACA pressures at 330 seconds (around lysis completion) differ by less than 0.01 %. Nevertheless, the finest mesh is used for more detailed lysis patterns. For spatial interpolation, a linear scheme is adopted for all simulations.

Results are saved every 2 to 10 seconds of simulation time depending on the phase of simulation, i.e., more frequent data acquisition during clot dissolution. All simulations start with zero pressure and velocity in the whole computational domain at the initial time $t = 0$. Initial concentrations of tPA, PLG, PLS and AP are 7×10^{-5} [8], 2 [9], 0 [9] and 1 [10] μM, respectively.

Further details regarding the OpenFOAM solver settings and case files are available upon request.

References

[1] Gibo H, Carver CC, Rhonton Jr. AL, Carla L, Mitchell RJ. Microsurgical anatomy of the middle cerebral artery. J Neurosurg 1981;54:151–69.

[2] Piebalgs A, Gu B, Roi D, Lobotesis K, Thom S, Xu XY. Computational Simulations of Thrombolytic Therapy in Acute Ischaemic Stroke. Sci Rep 2018;8:15810. doi:10.1038/s41598-018-34082-7.

[3] Blanco PJ, Watanabe SM, Passos MARF, Lemos PA, Feijóo RA. An anatomically detailed arterial network model for one-dimensional computational hemodynamics. IEEE Trans Biomed Eng 2015;62:736–53. doi:10.1109/TBME.2014.2364522.

[4] Pirola S, Menichini C, Guo B, Saitta S, Fu W, Dong Z, et al. 4D Flow MRI-Based Computational Analysis of Blood Flow in Patient-Specific Aortic Dissection. Trans Biomed Eng 2009. doi: 10.1109/TBME.2019.2904885

[5] Ogoh S. Middle cerebral artery flow velocity and pulse pressure during dynamic exercise in humans. AJP Hear Circ Physiol 2004. doi:10.1152/ajpheart.00979.2004.

[6] Matano F, Murai Y, Tanikawa R, Kamiyama H, Tateyama K, Tamaki T, et al. Intraoperative middle cerebral artery pressure measurements during superficial temporal artery to middle cerebral artery bypass procedures in patients with cerebral atherosclerotic disease. J Neurosurg 2016. doi:10.3171/2015.10.JNS151305.

[7] Bivard A, Lin L, Parsonsb MW. Review of Stroke Thrombolytics. J Stroke 2013;15:90. doi:10.5853/jos.2013.15.2.90.

[8] Booth NA. Fibrinolysis and thrombosis. Bailliere's Best Pract Res Clin Haematol 1999. doi:10.1053/beha.1999.0034.

[9] Anand S, Diamond SL. Computer simulation of systemic circulation and clot lysis dynamics during thrombolytic therapy that accounts for inner clot transport and reaction. Circulation 1996;94:763–74. doi:10.1161/01.CIR.94.4.763.

[10] Cederholm-Williams SA. Concentration of plasminogen and antiplasmin in plasma and serum. J Clin Pathol 1981. doi:10.1136/jcp.34.9.979.